Polymer Chemistry

Modulating the Crystallinity, Mechanical Properties, and Degradability of Poly(ε-caprolactone) Derived Polyesters by Statistical and Alternating Copolymerization

Journal:	*Polymer Chemistry*
Manuscript ID	PY-ART-02-2019-000274.R1
Article Type:	Paper
Date Submitted by the Author:	07-Apr-2019

Complete List of Authors:	Liu, Qianhui; The University of Akron, Polymer Science Yuan, Shichen; The University of Akron, Polymer Science Guo, Yuanhao; The University of Akron, Polymer Engineering Narayanan, Amal; The University of Akron, Department of Polymer Science Peng, Chao; The University of Akron, Polymer Science Wang, Shijun; The University of Akron, Polymer Science Miyoshi, Toshikazu; University of Akron , Polymer Science Joy, Abraham; The University of Akron, Polymer Science

ARTICLE

Modulating the Crystallinity, Mechanical Properties, and Degradability of Poly(ε-caprolactone) Derived Polyesters by Statistical and Alternating Copolymerization

Received 00th January 20xx,
Accepted 00th January 20xx

DOI: 10.1039/x0xx00000x

Qianhui Liu[a], Shichen Yuan[a], Yuanhao Guo[b], Amal Narayanan[a], Chao Peng[a], Shijun Wang[a], Toshikazu Miyoshi[a], Abraham Joy[a,*]

Poly(ε-caprolactone) (PCL) is a widely used biomaterial, but the long degradation time and hydrophobicity limit its applications in instances where short-term usage is needed. Synthesis of PCL analogues is an active area of research, but is constrained by the detailed and stringent synthetic procedures involved in the synthesis and polymerization of the cyclic lactones. Here we report a simple route to PCL analogues by copolymerizing PCL oligomer diol with a hydrogen bonding monomer diol and succinic acid in both statistical and alternating sequences. As a control, a homo-polyester from PCL oligomer diol and succinic acid was synthesized as well. The incorporation of the hydrogen bonding diol in different distributions results in correspondingly distinct polymer properties. The introduction of the hydrogen bonding monomer disrupts the microstructure of PCL which results in lower crystallinity, melting point and Young's modulus, but a more distinct strain hardening. The statistical distribution of the hydrogen bonding monomer along the polymer backbone accelerates the hydrolytic degradation rate.

Introduction

Poly(ε-caprolactone) (PCL) has been one of the most widely used biomaterials for fabricating medical devices,[1-3] tissue engineering devices,[4-7] and drug releasing applications due to its mechanical properties, ease of synthesis, and biocompatibility.[8-11] However, there are several drawbacks of PCL that prevent its adoption for additional biomedical needs. For instance, the long degradation time (2-5 years) prevents its use when faster degradation times are required, and the hydrophobic nature of PCL restricts the facile release of hydrophobic drugs.[8] The lack of mechanical strength in high load bearing applications prevents its use in bone plates, screws, and nails.[12] Also, the lack of functional groups on PCL precludes conjugation of ligands for enhancing the biological responses. Providing a facile methodology for the modification of PCL is a valuable approach to modulate properties such as crystallinity, hydrophilicity and mechanical properties, and would further increase the use of PCL in various applications. Herein, we describe a facile method for incorporation of functional groups in PCL diol-based polycondensations to provide statistical and alternating copolymers. Such modified PCL analogues acquire useful changes in their mechanical properties, hydrolytic degradation and crystalline structures compared to the native PCL-diol based polyester. The ease of synthesis of such analogues is likely to accelerate the adoption of this strategy to obtain modified PCL.

It has been reported that PCL can be modified either through physical[13-17] or chemical means. The chemical modification of PCL can be achieved by using monomers with various functional groups, copolymerization and post-functionalization. In the first category, ε-caprolactone (CL) functionalized with functional groups such as protected hydroxyl,[18-19] alkane,[20] alkyne,[21] and halogen[19, 22-23] has been reported.[24] The functional groups are commonly introduced at the γ-, α- or ε-position of CL,[25] but Winkler *et al*.[26] have also functionalized the β-position of CL monomer. However, both functional monomer synthesis and their polymerization are synthetically tedious, require multiple steps, and often involve multiple protection and deprotection of the functional groups.[27] Copolymerization of PCL with other polymers, or copolymerization of CL with other monomers is another approach to introduce functionality. Synthesis of block,[28-33] graft,[34-39] random[40] and alternating[41-43] copolymers of PCL has been reported. The random copolymers are generally achieved by ring-opening polymerization of various lactones with reactivity ratio of ~ 1:1. As an illustration, Malhotra *et al*.[44] developed an amphiphilic random copolymer by ring opening copolymerization of hydrophobic CL and hydrophilic carboxylic acid-functionalized CL. Examples of PCL derived alternating copolymers include small monomers or oligomers arranged in an alternating sequence. For instance, Sharma and coworkers[45] developed an alternating poly(amide urethane) from ε-caprolactone, diamines, and diphenyl carbonate. Li *et al*.[46] obtained alternating block polyurethanes from PEG diol, hexamethylene diisocyanate and PCL diol.

[a] *Department of Polymer Science, The University of Akron, Akron, Ohio, 44325, USA*
[b] *Department of Polymer Engineering, The University of Akron, Akron, Ohio, 44325, USA*
Email: Abraham@uakron.edu
Electronic Supplementary Information (ESI) available: [details of any supplementary information available should be included here]. See DOI: 10.1039/x0xx00000x

Post-functionalization can be performed on unmodified PCL, or together with the other two functionalization methods mentioned above. The direct functionalization of PCL is hard to carry out, although still possible. Xu *et al* functionalized PCL film by incorporating glycidyl methacrylate polymer brushes through surface-initiated atom transfer radical polymerization.[47] Parrish and coworkers copolymerized ε-CL and α-propargyl-δ-valerolactone in a statistical manner, and the polymer was further functionalized through azide-alkyne click reaction.[48]

In this work, we present a facile step-growth copolymerization of PCL oligomer diol (M_n: 2000 Da) (not monodispersed) with N-functionalized serinol monomers and succinic acid to provide both statistical and alternating copolymers. Our lab has reported a library of N-functionalized diethanolamine derived diols containing a variety of functional pendent groups such as phenyl, amine, alkene, and alkyne groups.[49] Thus there are multiple choices to functionalize PCL with this method. As an illustration, a monomer containing two hydrogen bonding secondary amide-propyl groups[50] was used in this work to modulate the PCL properties. As a control, a homo-polyester from PCL oligomer diol and succinic acid was synthesized to show the unique properties brought by the hydrogen-bonding monomer. Statistical and alternating copolyesters were synthesized to show that different physical and chemical properties can be achieved by regulating the distribution of the small monomer along the backbone, even though the chemical structures are the same.

Experimental

Materials

Serinol was purchased from Oakwood Chemical. 4-aminobutyric acid and PCL oligomer diol with number average molecular mass (M_n) of 2000 *Da* were purchased from Acros Organics. Thionyl chloride and triethylamine (TEA) were purchased from EMD Millipore Corporation. Butyric anhydride, 1,4-dioxane, and succinic anhydride were purchased from Alfa Aesar. Succinic acid, methanol, and dichloromethane were purchased from Fisher Chemical. N,N'-diisopropylcarbodiimide (DIC) and 4-dimethylaminopyridine (DMAP) were purchased from Chem Impex International Inc. 4-(dimethylamino) pyridinium-4-toluene sulfonate (DPTS) and the diol containing 2 amide-propyl groups were synthesized based on previous reports.[51,50]

Analytical methods

^{1}H and ^{13}C NMR spectra were recorded by a Varian NMR instrument (300 MHz). Chemical shifts were reported in ppm relative to solvent residue signal (^{1}H NMR $CDCl_3$ 7.27 ppm, ^{13}C NMR $CDCl_3$ 77.16 ppm). Number average (M_n) and weight average (M_w) molecular masses, and dispersity (*Đ*) were obtained by a size exclusion chromatography (SEC). THF was used as eluent, with the flow rate of 1 mL/min and temperature of 40 °C. SEC was performed on a TOSOH HLC-8320 GPC equipped with refractive index detector, and polystyrene standards with M_n varying from 500 Da to 5480000 Da were used for calibration. Thermogravimetric analysis (TGA) was performed on a TA Q500 TGA instrument from room temperature to 600 °C with a heating rate of 10 °C /min under N_2 atmosphere, to obtain the thermal decomposition temperature (T_d). Melting point (T_m) and crystallization point (T_c) were obtained from differential scanning calorimetry (DSC) with a scanning rate of 10 °C /min under N_2 atmosphere. Glass transition temperature (T_g) and melting point (T_m) were obtained from dynamic mechanical analysis (DMA) at a frequency of 1 Hz, a strain of 0.2 %, and a ramp rate of 3 °C /min. The temperature where loss modulus (E'') reached the peak denoted T_g, and the temperature where storage modulus (E') dramatically dropped was regarded as T_m.

Synthesis of the hydrogen bonding monomer diol containing 2 amide groups (A)[50]

4-Aminobutyric acid (10.3 g, 99.6 mmol) was dissolved in anhydrous MeOH (120 mL), followed by the addition of thionyl chloride (18.08 mL, 249 mmol) via an additional funnel at 0 °C. After 30 min, the reaction was carried out at room temperature overnight. Solvent and the excess of thionyl chloride were removed under vacuum to give a white solid. The crude product was used without further purification.

Methyl-4-aminobutyrate from the previous step (16.6 g, 96 mmol) and a mixture of water (15 mL) and dioxane (45 mL) were added into a round bottom flask equipped with a stir bar. TEA (24.3 g, 240 mmol) was added at 0 °C. Butyric anhydride (38 g, 240 mmol) in a mixture of water (10 mL) and dioxane (30 mL) was added dropwise into the round-bottom flask. The reaction was carried out at room temperature overnight open to the atmosphere. Solvents were removed under vacuum and the residue was poured into saturated $NaHCO_3$ solution (500 mL) overnight with vigorous stirring. The product was extracted with ethyl acetate (60 mL, 3×) followed by washed with saturated $NaHCO_3$ (50 mL, 2×), brine (50 mL, 1×) and dried over Na_2SO_4. The organic phase was concentrated under vacuum to give a white solid (16.33 g, 91%).

^{1}H NMR (300 MHz, $CDCl_3$), δ (ppm): 0.95 (t, J=7.5 Hz, 3H), 1.60 – 1.72 (m, 2H), 1.85 (quin, J=6.75 Hz, 2H), 2.14 (t, J=7.5 Hz, 2H), 2.38 (t, J=7.5 Hz, 2H), 2.30 (q, J=7 Hz, 2H), 3.68 (s, 3H), 5.70 (br.s, 1H).

Methyl 4-butanamidobutanoate from the second step (13.0 g, 69.5 mmol) and serinol (9.4 g, 103.2 mmol) were added into a 200 mL round-bottom flask and the reaction was carried out at 80 °C under vacuum overnight. The monomer was purified by silica column chromatography (20 % MeOH, 80 % DCM, R_f = 0.3) to give a white solid (17.42 g, 81 %).

^{1}H NMR (300 MHz, DMSO-d_6), δ (ppm): 0.84 (t, J=7.5 Hz, 3H), 1.44 – 1.56 (m, 2H), 1.59 (quin, J=7.5 Hz, 2H), 2.02 (t, J=7.5 Hz, 2H), 2.07 (t, J=7.5 Hz, 2H), 3.01 (q, J=6 Hz, 2H), 3.38 (t, J=6 Hz, 4H), 3.64 – 3.75 (m, 1H), 4.55 (t, J=6 Hz, 2H), 7.44 (d, J=9 Hz, 1H), 7.72 (t, J= 9 Hz, 1H). ^{13}C NMR (300 MHz, DMSO-d_6), δ (ppm): 13.63 (s), 18.69 (s), 25.59 (s), 32.97 (s), 37.41 (s), 38.05 (s), 52.82 (s), 60.26 (s), 171.77 (s), 171 89 (s). ESI-MS ($[M+Na]^+$): 269.2 (calc.: 246.2).

Synthesis of PCL oligomer diacid (SCS)

PCL oligomer (**C**) diol with M_n of 2000 *Da* (15.00 g, 7.5 mmol) was completely dissolved in anhydrous DCM (20 mL) in a 250 mL one-neck round bottom flask, followed by succinic anhydride (1.801 g, 18 mmol) and DMAP (0.183 g, 1.5 mmol) were added into the flask. The reaction was carried out at 30 °C for 15 h, and the reaction mixture turned to a white suspension due to the precipitating DMAP salt. Additional DCM was used to transfer the mixture to a separation funnel and HCl solution (1 M, 100 mL) was used to wash

the organic layer. The solution was dried over Na_2SO_4, and the solvent was removed under reduced pressure. The product was completely dried in a high vacuum oven. NMR and ESI mass spectroscopy were used to corroborate that the conversion is 100 %.

^{1}H NMR (300 MHz, $CDCl_3$), δ (ppm): 1.36 – 1.43 (m, 40H), 1.60 – 1.67 (m, 80H), 2.28 – 2.35 (m, 40H), 2.64 – 2.66 (m, 8H), 3.69 (t, J=6 Hz, 4H), 4.04 – 4.12 (m, 40H), 4.23 (t, J=4.5 Hz, 4H).

Synthesis of P(CS)

C diol with M_n of 2000 Da (1.540 g, 0.77 mmol), succinic acid (**S**) (0.091 g, 0.77 mmol), and DPTS (0.090 g, 0.31 mmol) were added into a 100 mL one-neck round bottom flask equipped with a magnetic stir bar. Anhydrous DCM (5 mL) was added into the flask under dry N_2. DIC (0.36 mL, 2.31 mmol) was added dropwise with cooling of an ice bath. The ice bath was withdrawn after 30 minutes, and the reaction allowed to proceed for 12 h at room temperature. The polymer was isolated from the cloudy reaction mixture by precipitating in MeOH three times to obtain the polymer, which was and dried completely in a high vacuum oven. The chemical structure was confirmed by NMR.

^{1}H NMR (300 MHz, $CDCl_3$), δ (ppm): 1.34 – 1.44 (m, 40H), 1.59 – 1.71 (m, 80H), 2.25 – 3.38 (m, 40H), 2.62 (s, 4H), 3.70 (t, J=4.5 Hz, 4H), 4.00 – 4.13 (m, 40H), 4.24 (t, J=4.5 Hz, 4H).

Synthesis of P(CS-stat-AS)

C diol with M_n of 2000 Da (1.5 g, 0.75 mmol), **A** diol (0.185 g, 0.75 mmol), succinic acid (**S**) (0.177 g, 1.5 mmol), and DPTS (0.175 g, 0.6 mmol) were added into a 100 mL one neck round bottom flask equipped with a magnetic stir bar. After the addition of anhydrous DCM (5 mL), DIC (0.704 mL, 4.5 mmol) was added dropwise with cooling of an ice bath. The reaction and purification procedures were the same as those for **P(CS)**.

^{1}H NMR (300 MHz, $CDCl_3$), δ (ppm): 0.94 (t, J=6 Hz, 3H), 1.33 – 1.43 (m, 40H), 1.60 – 1.71 (m, 80H), 1.79 – 1.84 (m, 4H), 2.15 (t, J=7.5 Hz, 2H), 2.25 (t, J=7.5 Hz, 2H), 2.29 – 2.38 (m, 40H), 2.64 (s, 8H), 3.28 (2H), 3.68 – 3.71 (t, J=4.5 Hz, 4H), 4.01 – 4.11 (m, 40H), 4.14 – 4.30 (m, 8H), 4.47 (1H).

Synthesis of P(CS-alt-AS)

SCS diacid (1.6 g, 0.727 mmol), **A** diol (0.179 g, 0.727 mmol), and DPTS (0.085 g, 0.291 mmol) were added into a 100 mL one neck round bottom flask with a magnetic stir bar. Anhydrous DCM (5 mL) was added, and DIC (0.34 mL, 2.18 mmol) was added dropwise with cooling of an ice bath. The rest of the procedures were the same as those for **P(CS)**.

^{1}H NMR (300 MHz, $CDCl_3$), δ (ppm): 0.93 (t, J=7.5 Hz, 3H), 1.33 – 1.43 (m, 40H), 1.60 – 1.70 (m, 80H), 1.76 – 1.85 (m, 4H), 2.14 (t, J=7.5 Hz, 2H), 2.24 (t, J=7.5 Hz, 2H), 2.28 – 2.37 (m, 40H), 2.63 (s, 8H), 3.28 (q, J=6 Hz, 2H), 3.67 – 3.71 (t, J=6 Hz, 4H), 4.06 (t, J=7.5 Hz, 40H), 4.14 – 4.30 (m, 8H), 4.47 (1H), 6.12 (1H), 6.84 (d, J=9Hz, 1H).

Mechanical property measurements

Tensile tests were performed on Instron 5530 with load cell of 100 N at 22 °C and 37 °C to study the mechanical properties of the three polymers. Polymer thin films with thickness of 0.5 mm were made with a vacuum compression moulding machine (TMP technical Machine Products Corp.). After moulding, the polymer films were taken out from the machine, cooled in ambient environment for 1 h, and then stored at 4 °C.

A die with half the size of type V specimen according to ASTM 638-2003[52] was used to make dogbone shaped specimens from polymer thin films. The accurate thickness and width of each specimen were measured by a calliper before the test. The speed of crosshead was set as 3 mm/min. For the test performed at 37 °C, specimens were kept isothermal for 10 min before stretching. The two ends of polymer specimens were wrapped with sand paper to prevent slippage between specimen and clamps. Reported data are based on triplet results of each sample under individual testing conditions.

Water contact angle measurement

Polymer thin films were obtained by spin coating the filtered polymer solutions (20 mg polymer in 1 mL toluene) on glass cover slips. The coated cover slips were placed in a fume hood for 2 h and then transferred to a high vacuum oven with temperature ~ 60 °C overnight. The cover slips were kept in ambient environment for 1h and then transferred to a fridge at 4 °C until tested. Water contact angles were measured by a contact angle goniometer (Ramé-Hart). The change of contact angle for the ultrapure water droplet (10 μL) on the surface was recorded by a camera every 10 s for 2 min.

Hydrolytic degradation test

Polymer films were obtained through compression moulding. Each testing sample with dimensions of 4 mm × 4 mm × 0.5 mm was kept in a 20 mL vial containing 15 mL of phosphate buffered saline (PBS) at 37 °C. There were three replicates of each sample. At specific intervals, samples were taken out of the buffer solution, washed with MeOH and dried in a high vacuum oven. Molecular mass of each testing sample was measured by SEC. The change of molecular mass was recorded and plotted against time.

Wide angle X-ray diffraction (WAXD)

Strip specimens were cut from polymer thin films by compression moulding, and were used for the wide angle X-ray diffraction test. WAXD experiments were performed on the instrument equipped with a Rigaku Rapid II sealed tube generator (X-ray wavelength is 0.154 nm) and an image plate as the detector. The working voltage and current were 40 kV and 30 mA, respectively, and the scanning time was 15 min. The sample template was aligned to make the X-ray beam parallel to the template plane. The 1D WAXD curve was integrated from the 2D image, peak fitting was done with Gaussian model using Origin 9.0 to assign crystalline peaks and amorphous halo, and the degree of crystallinity was calculated.

During tensile testing, three polymers were stretched to a strain of 25 mm/mm and fixed, and the middle part of the stretched specimen was cut and characterized by WAXD to study orientation of crystals (the cut specimens were kept in dry ice while transferring to the WAXD to minimize the relaxation of polymer chains, and WAXD was run immediately). The Azimuthal profile of the two peaks on the 2D-WAXD patterns was calculated by integrating the two isotropic rings with 2θ in the range of [20 °, 22 °] and [22.5 °, 25 °]. The detailed calculations of the Herman's orientation factor of the crystal are provided in the supplementary information.

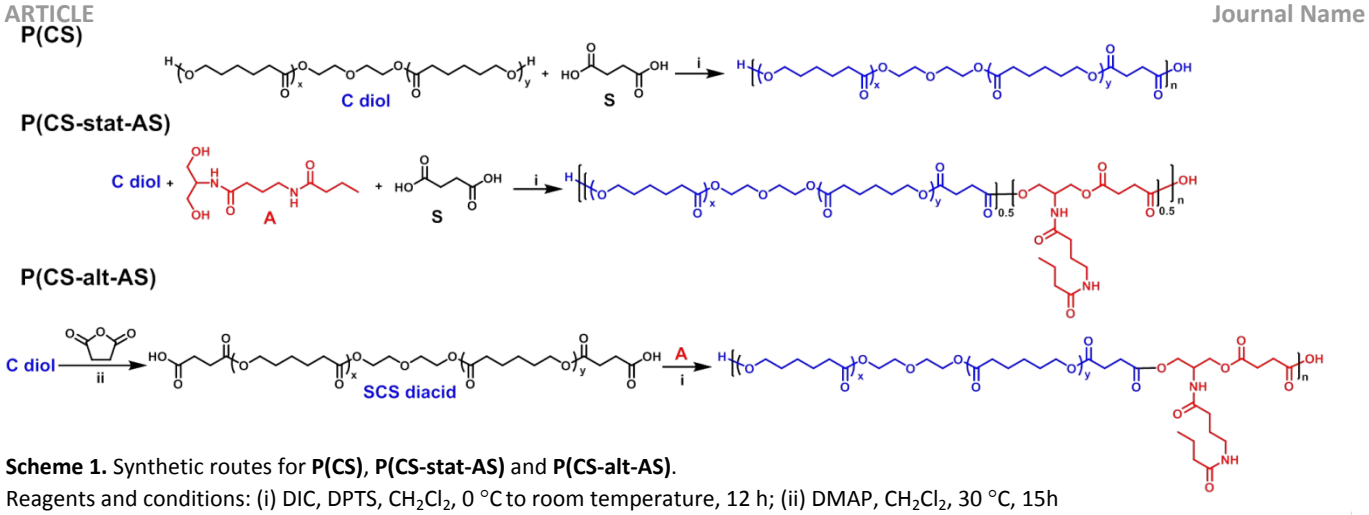

Scheme 1. Synthetic routes for **P(CS)**, **P(CS-stat-AS)** and **P(CS-alt-AS)**.
Reagents and conditions: (i) DIC, DPTS, CH_2Cl_2, 0 °C to room temperature, 12 h; (ii) DMAP, CH_2Cl_2, 30 °C, 15h

Results and discussion

Polymer synthesis

The synthesis of 'peptide-like' polyesters by carbodiimide coupling of diols and diacids under mild reaction conditions were reported by Gokhale *et al*.[49] Peng reported the synthesis of an alternating copolyester by reacting a diol from *N*-functionalized diethanolamide with a diacid derived from *N*-functionalized diethanolamide.[53] In this work, polyesters were synthesized using a similar synthetic method, as shown in **Scheme 1**. For synthesis of the statistical copolyester (**P(CS-stat-AS)**), PCL oligomer (**C**) diol with M_n of 2000 *Da*, the hydrogen bonding monomer (**A**) and succinic acid (**S**) were reacted together in one pot. For the alternating polyester (**P(CS-alt-AS)**), **SCS** diacid was made by reacting **C** diol with succinic anhydride, and it was then polymerized with **A** diol. As a control, a homo-polyester of **C** diol and **S** was synthesized (**P(CS)**). ^{1}H NMR spectroscopy confirmed the chemical structures as shown in **Figure 1**. For the homo-polyester **P(CS)**, protons from succinic acid (2.62 ppm) were set as reference and the integral value was set to 4. Integral values of protons from the ether group of the PCL segment (3.7 ppm) was 4, and it is consistent with the chemical structure. For **P(CS-stat-AS)** and **P(CS-alt-AS)**, integral value of protons from succinic acid (2.61 – 2.64 ppm) was set to 8. Protons in the backbone adjacent to the secondary amide group (~ 4.48 ppm) gave an integral value ~ 1, and the ether protons from PCL segment (3.68 – 3.71ppm) gave an integral value of ~ 4. This indicated that the molar ratio of PCL segment to **A** diol segment was almost 1:1 in the obtained polyesters, which was in accordance with the feed ratio. Peak picking, integration and insets of small peaks for the three polymers are available in **Figure S1**. A unimodal molecular mass distribution was observed from SEC curve of each polymer (**Figure S2**), proving the formation of copolyester, instead of mixtures of homo-polyesters.

Molecular characterization and thermal properties

The three polyesters have similar molecular masses (M_n ~ 80 kDa) and dispersity ($Đ$ ~ 2). In the DSC, the temperature was raised to 80 °C, decreased to -20 °C, and increased to 80 °C again. T_c and T_m were obtained from the 2nd and the 3rd cycle, respectively. The onset T_m was determined by the intercept of the tangent of the peak with the extrapolated baseline as shown in **Figure S3**. **P(CS)** and **P(CS-alt-AS)** have the highest and lowest onset and peak T_m, as

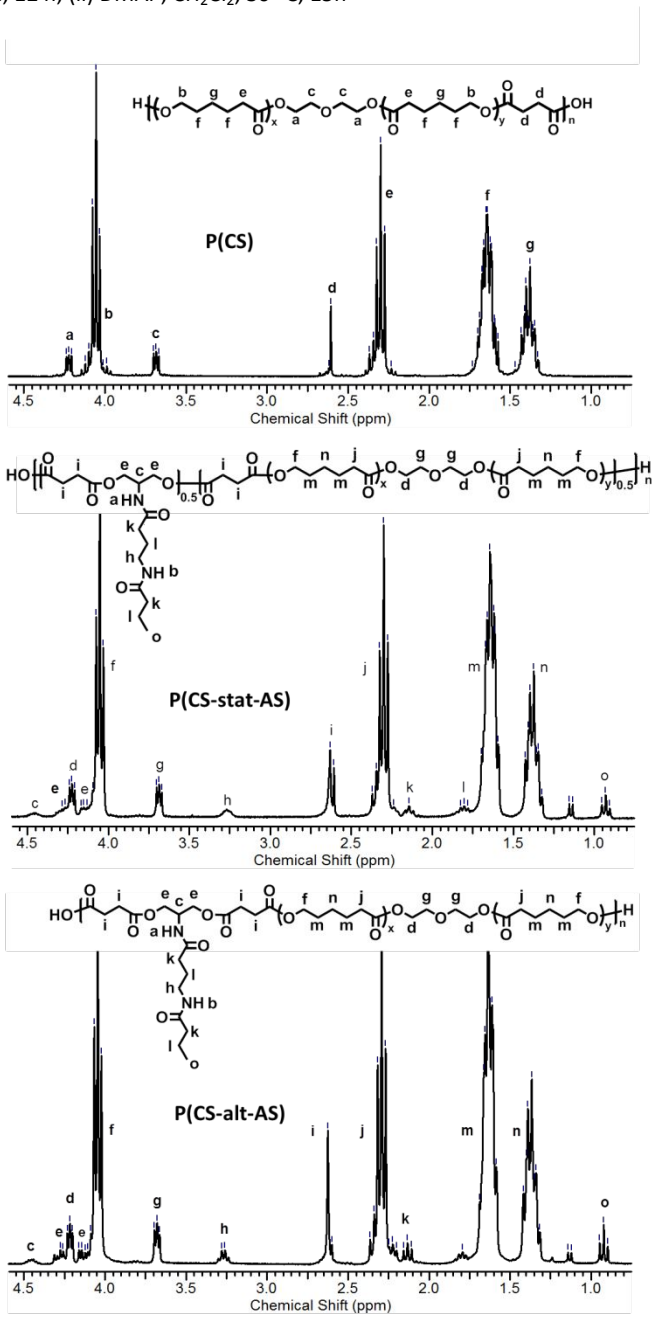

Figure 1. ^{1}H NMR spectra of **P(CS)**, **P(CS-stat-AS)** and **P(CS-alt-AS)** in $CDCl_3$.

Table 1. Number average molecular mass (M_n), dispersity ($Đ$), melting point (T_m), glass transition temperature (T_g), thermal decomposition temperature (T_d), and degree of crystallinity of **P(CS)**, **P(CS-stat-AS)**, and **P(CS-alt-AS)**

Sample	M_n[a]	$Đ$[a]	$T_{m,onset}$[b]	$T_{m,peak}$[b]	T_m[c]	T_g[c]	T_d[d]	crystallinity[e]
	(kDa)		(°C)	(°C)	(°C)	(°C)	(°C)	(%)
P(CS)	77.8	1.91	39	41	57	-46	307	39
P(CS-stat-AS)	77.2	1.89	30	40	53	-40	232	33
P(CS-alt-AS)	77.9	1.93	24	35	51	-36	250	26

[a] Determined by SEC with THF as the eluent and PS as the standard. [b] Determined by DSC using a heating/cooling rate of 10 °C /min. [c] Determined by DMA with the frequency of 1 Hz, strain of 0.2 %, and ramp rate of 3 °C /min. [d] Determined by TGA with the heating rate of 10 °C /min. [e] Determined by peak fitting of WAXD figure.

well as T_c, respectively. The introduction of hydrogen bonding monomer diol disrupts the order of the crystallizable PCL chains, especially for **P(CS-alt-AS)**. Yet, in **P(CS-stat-AS)**, there are longer stretches of PCL leading to more crystalline regions compared with **P(CS-alt-AS)**. In the DMA test, the temperature was increased from -80 °C to 60 °C with a ramp rate of 3 °C/min. The temperature at the peak of E'' denotes T_g, and the temperature where E' starts to drop dramatically denotes T_m (**Figure S4**). The temperature at E'' peak is selected as T_g because it closely relates to the physical property changes due to the glass transition. The selection is consistent with the concept that T_g is the temperature where segments start to move. DMA shows that **P(CS)** and **P(CS-alt-AS)** have the lowest and highest T_g, of -46 and -36 °C, respectively, and **P(CS-stat-AS)** has an intermediate T_g at -40 °C, based on the *E''* peak. Compared to the T_g value of **P(CS)**, the introduction of the diol containing two amide groups in the side chain increases the T_g. The side chain containing two secondary amide groups is polar, and H-bonds can form between secondary amide groups,[50] which increase interactions among polymer chains and lead to higher T_g. Especially in the case of **P(CS-alt-AS)**, where the interaction is more evenly distributed along polymer chains, the T_g increased by 10 °C compared to **P(CS)**. Melting points measured from dynamic mechanical analysis (DMA) are around 15 °C higher than those obtained from DSC, and the melting points of **P(CS)** and **P(CS-alt-AS)** from DMA are the highest and lowest, respectively, which is consistent with the result from DSC. Degree of crystallinity was obtained from wide angle X-ray diffraction. Three typical peaks of PCL corresponding to crystal planes of (110), (111), and (200) and an amorphous halo were observed on the WAXD pattern (**Figure S7(a)**). The degree of crystallinity of the three polymers was determined by peak fitting of the crystalline peak and the amorphous halo with Gaussian model using Origin 9.0. **P(CS)** shows the highest degree of crystallinity ~ 39 % and **P(CS-alt-AS)** has the lowest degree of crystallinity ~ 26 % (**Figure S8**). This result is consistent with melting points of the three polyesters. The molecular and thermal properties of the three polymers are summarized in **Table 1**.

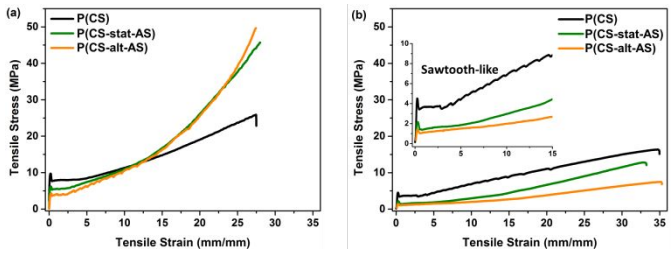

Figure 2. Stress-strain curves for **P(CS)**, **P(CS-stat-AS)** and **P(CS-alt-AS)** at (a) 22 °C and (b) 37 °C.

Mechanical properties and chain orientation

Tensile testing of the three polyesters was carried out at 22 °C and 37 °C. Dogbone shaped specimens with half the size of type V specimen according to ASTM 638-2003[52] were used. At 22 °C, **P(CS)** showed the highest Young's modulus and yield stress of 110.8 MPa and 9.5 MPa, respectively. **P(CS-stat-AS)** showed a Young's modulus of 68.2 MPa and yield stress of 6.1 MPa. **P(CS-alt-AS)** with the lowest degree of crystallinity has the lowest Young's modulus and yield stress, which are 36.6 MPa and 4.8 MPa, respectively (**Figure 2(a)**). The degree of crystallinity is important in determining mechanical properties, especially for moduli and yield stress. The trend in this work shows that the polyester with higher degree of crystallinity has higher modulus and yield stress, which is consistent with the references.[54-56] Molecular mass plays a significant role in determining strain at break and strain hardening.[54-55] All three polyesters used in this work have similar molecular masses, and they show similar strains at break at ~ 28 mm/mm. It should be noted that the extensometer was not able to be used due to the very small specimen size. The length of narrow section according to

Table 2. Summary of mechanical properties of **P(CS)**, **P(CS-stat-AS)** and **P(CS-alt-AS)** at 22 °C and 37 °C

Sample at 22 °C	Ultimate strength (MPa)	Strain at break (mm/mm)	Young's modulus (MPa)	Yield stress (MPa)
P(CS)	27.1 ±	30.1 ± 2.4	110.8 ±	9.5 ±
P(CS-stat-AS)	42.7 ±	27.4 ± 0.7	68.2 ± 4.2	6.1 ±
P(CS-alt-AS)	44.8 ±	28.4 ± 1.4	36.6 ± 6.9	4.8 ±

Sample at 37 °C	Ultimate strength (MPa)	Strain at break (mm/mm)	Young's modulus (MPa)	Yield stress (MPa)
P(CS)	16.0 ±	34.4 ± 0.4	38.2 ±	4.4 ±
P(CS-stat-AS)	11.7 ±	32.3 ± 1.8	15.3 ±	2.0 ±
P(CS-alt-AS)	7.1 ± 1.0	32.8 ± 2.0	9.9 ± 1.3	1.5 ±

ASTM D 638-2003 (4.8 mm) was used as the initial length. However, the experimental error in strain was inevitable since the wide parts on the dogbone shaped specimens got stretched as well.

P(CS) has the least strain hardening with the ultimate strength of 27.1 MPa, while introduction of hydrogen bonding monomer results in distinct strain hardening. **P(CS-alt-AS)** and **P(CS-stat-AS)** show ultimate strength of 44.8 and 42.7 MPa, respectively. A similar strain hardening phenomenon was observed by Winey with a carboxyl functionalized polyethylene (PE)-derivative.[56] With in-situ XRD, they observed that the initial isotropic acid-rich layers/aggregates were disrupted during stretching because of the weak hydrogen bonds, and aligned with PE layers perpendicular to the draw direction. A possible reason of strain hardening for **P(CS-stat-AS)** and **P(CS-alt-AS)** in this work is that the H-bonded amide-rich layers/aggregates align perpendicular to the draw direction, and this structure progressively aligns during elongation. The increase of degree of crystallinity during stretching could be another reason. The 1D WAXD figures of the specimens before and after tensile testing are shown in **Figure S7**. However, due to the unavailability of in-situ WAXD and lack of appropriate references, it was difficult to assign peaks for the WAXD patterns on samples post-tensile testing. Therefore, the presence of amide-rich layer perpendicular to the elongation direction, and the increase of degree of crystallinity are probable reasons for the observed strain-hardening.

Two strong diffraction patterns at 2θ = 21.4 ° and 23.7 ° are observed in the 2D WAXD image (**Figure 3 and Figure S7**), which are assigned to (110) and (200) plane,[57] respectively. They are very close to the 2θ values of the crystal of PCL, hence the introduced pendant groups do not affect the crystalline structure of PCL.[57] As shown in **Figure 3**, after tensile testing, the two strong patterns are concentrated from isotropic rings to arcs, especially for **P(CS)** which shows the narrowest arc, due to the orientation of the crystals. The *c** axis of the crystals tends to orient along the stretching direction (Z direction) under tension. A quantitative measure of uniaxial orientation can be presented using Herman's orientation factor ($f_{c,z}$).[58] $f_{c,z}$ is equal to 1 when chains are perfectly aligned with the reference axis (z direction in this work), and $f_{c,z}$ is 0 when chains have random orientation.[59] The details of the calculation of the Herman's orientation factors are shown in the supplementary information. **Figure 3** shows that **P(CS)** and **P(CS-stat-AS)** have the highest and lowest orientation factors of 0.81 and 0.65, respectively. This suggests that the best orientation of crystals is achieved in the control polymer without the interruption of hydrogen bonding monomer diol. Incorporation of the diol monomer reduced crystal orientation, and a better orientation was observed in the alternating polymer compared to the statistical one.

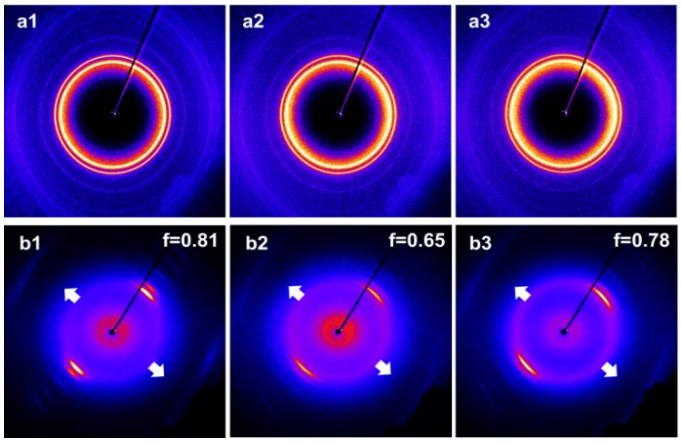

Figure 3. WAXD 2D images of **P(CS)** (a1, b1), **P(CS-stat-AS)** (a2, b2) and **P(CS-alt-AS)** (a3, b3) before and after tensile testing at room temperature. Herman's orientation factors of **P(CS)**, **P(CS-stat-AS)** and **P(CS-alt-AS)** are 0.81, 0.65 and 0.78, respectively, after stretching. Arrows indicated sample stretching direction.

As we expect the modified PCL to be used in applications such as drug releasing materials and scaffolds in tissue engineering, the tensile testing of the polymers was performed at 37 °C as well. At 37 °C, the strain at break increased, while Young's modulus, yield stress and ultimate strength decreased for the three polymers, as shown in **Figure 2(b)**. Furthermore, the remarkable strain hardening was not observed in either copolyester. This may be due to the decrease of crystalline content, especially for **P(CS-stat-AS)** and **P(CS-alt-AS)** with low melting points. The two copolyesters started to melt when kept isothermal at 37 °C. Mechanical properties of all samples at 22 °C and 37 °C are summarized in **Table 2**.

It is worth noting that in the stress-strain curves, a sawtooth-like profile appears for all three polyesters under specific conditions. For instance, the sawtooth profile arises for **P(CS-alt-AS)** at room temperature (**Figure 2(a)**), and for **P(CS)** at 37 °C (**Figure 2(b)**), with a strain rate of 3 mm/min. Tensile testing for the three polyesters was expanded to different temperatures (18, 22, 28, 32, 37, and 40 °C) (**Figure S5**), and it showed that the sawtooth appeared for all polyesters, but only in a temperature range close to the melting point of the polyester. In addition, tensile testing using various strain rates (0.75 mm/min, 3 mm/min and 12 mm/min) was carried out for **P(CS-stat-AS)** at 32 °C, and the sawtooth profile only appeared at low tensile rates (0.75 and 3 mm/min) (**Figure S5**). Similar sawtooth-like profiles were observed in Ragaert's work for bulk PCL as the specimen entered strain-hardening region.[60] The authors observed tiered deformation of the broad part at two ends of the dogbone shaped specimen, which was considered to be the cause for the sawtooth-like profile. The tiered deformation at two ends of the specimen was not clearly observed in this work, while after breaking, the specimen showed a zigzag shape (**Figure S6**).

Water contact angle and hydrolytic degradation

It was expected that the copolyesters would be more hydrophilic than **P(CS)** since the monomer diol is hydrophilic and hygroscopic as confirmed in our previous report.[50] Yet, there was no significant difference among static water contact angles for the three polyesters (~ 80 °), and water does not spread on the surface of any polymer during the 2 min test window (**Figure 4(a)**). This is because the relatively hydrophobic PCL oligomer is much larger than the monomer diol in both copolyesters, and the effect of the monomer diol on increasing hydrophilicity is overshadowed.

PCL has a long hydrolytic degradation time of around 2-5 years,[61-62] which hinders its use in some short-term applications. The polymers examined here were incubated in PBS (pH=7.4) at 37 °C for 88 days, and the M_n of **P(CS)**, **P(CS-stat-AS)** and **P(CS-alt-AS)** reduced by 4 %, 35 % and 6 %, respectively, as shown in **Figure 4(b)**.

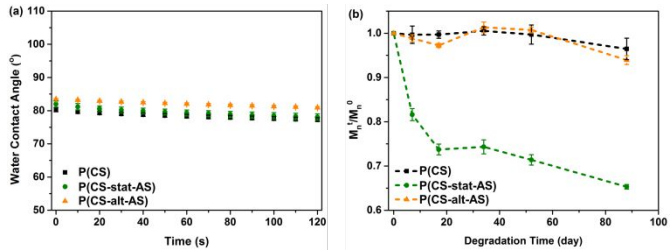

Figure 4. (a) Static water contact angle measurements for **P(CS)**, **P(CS-stat-AS)** and **P(CS-alt-AS)** during 2 min; (b) Decrease of M_n for **P(CS)**, **P(CS-stat-AS)** and **P(CS-alt-AS)** during hydrolytic degradation in PBS buffer (pH = 7.4)

P(CS-stat-AS) has a significant reduction in molecular mass compared to the other two polyesters. The secondary amide groups in the side chain can form H-bonds with water molecules, increasing the water content of the local environment. Due to the presence of the short homo-sequences of the hygroscopic diol in **P(CS-stat-AS)**, the molecular mass dropped sharply in the beginning, and then the degradation rate levelled off because of the decrease in the number of sites of the hydrophilic diols. No significant increase of degradation rate is observed with **P(CS-alt-AS)** even though the hydrogen bonding monomer diol is incorporated. This result can be attributed to homogeneity of the alternating polyester. Due to the hydrophobicity of PCL and lack of homo-sequences of the hydrophilic diols, water likely has a much slower rate of access to the polyester bulk (compared to **P(CS-stat-AS)**) to promote hydrolytic degradation. Similar degradation results were reported by Meyer[63] who showed that the molecular mass decreases faster with statistical PLGA compared to the alternating one.

Conclusion

This work presents a facile synthesis method to obtain PCL analogues by copolymerizing PCL oligomer diol with a hydrogen bonding monomer diol and succinic acid in both statistical and alternating sequences. The effects of the monomer diol and its distribution along backbone on polymer properties have been studied. **P(CS)** has the highest T_m and crystallinity, and hence the highest Young's modulus and yield stress. Incorporation of monomer diol disrupts the order of crystalline PCL, resulting in decreased crystallinity, T_m, Young's modulus, and yield stress, especially for **P(CS-alt-AS)**. However, **P(CS-stat-AS)** and **P(CS-alt-AS)** demonstrate more remarkable strain hardening and higher ultimate strength than **P(CS)**, potentially due to the formation and alignment of the hydrogen-bonded amide group-rich layer during tensile testing, and increase of degree of crystallinity during stretching. Crystals of all polyesters are isotropic before tensile testing, and **P(CS)** and **P(CS-stat-AS)** show the highest and lowest Herman's orientation factors, respectively, after tensile testing. **P(CS-stat-AS)** presents a significant increase in hydrolytic degradation rate compared to the other two polyesters. Apart from the hydrogen bonding monomer diol, a variety of other monomer diols containing different functional groups are available based on our previous reports. Specific diols can be incorporated to accomplish the desired polymer properties. Furthermore, post functionalization can be achieved by a conjugating group, such as azide or alkyne group, and hence this provides further opportunities to modify PCL.

Conflicts of interest

There are no conflicts to declare

Acknowledgement

This work was supported in part by an NSF Grant (NSF DMR # 1352485)

Notes and references

1. Middleton, J. C.; Tipton, A. J., Synthetic biodegradable polymers as orthopedic devices. *Biomaterials* **2000,** *21* (23), 2335-2346.
2. Jones, D. S.; Djokic, J.; McCoy, C. P.; Gorman, S. P., Poly(ε-caprolactone) and poly(ε-caprolactone)-polyvinylpyrrolidone-iodine blends as ureteral biomaterials: characterisation of mechanical and surface properties, degradation and resistance to encrustation in vitro. *Biomaterials* **2002,** *23* (23), 4449-4458.
3. Dhanaraju, M. D.; Jayakumar, R.; Vamsadhara, C., Influence of Manufacturing Parameters on Development of Contraceptive Steroid Loaded Injectable Microspheres. *Chemical and Pharmaceutical Bulletin* **2004,** *52* (8), 976-979.
4. Dong, L.; Wang, S.-J.; Zhao, X.-R.; Zhu, Y.-F.; Yu, J.-K., 3D- Printed Poly(ε-caprolactone) Scaffold Integrated with Cell-laden Chitosan Hydrogels for Bone Tissue Engineering. *Scientific Reports* **2017,** *7* (1), 13412.
5. Kim, Y. B.; Kim, G. H., PCL/Alginate Composite Scaffolds for Hard Tissue Engineering: Fabrication, Characterization, and Cellular Activities. *ACS Combinatorial Science* **2015,** *17* (2), 87-99.
6. Huang, A.; Jiang, Y.; Napiwocki, B.; Mi, H.; Peng, X.; Turng, L.-S., Fabrication of poly(ε-caprolactone) tissue engineering scaffolds with fibrillated and interconnected pores utilizing microcellular injection molding and polymer leaching. *RSC Advances* **2017,** *7* (69), 43432-43444.
7. Hasan, A.; Soliman, S.; El Hajj, F.; Tseng, Y.-T.; Yalcin, H. C.; Marei, H. E., Fabrication and In Vitro Characterization of a Tissue Engineered PCL-PLLA Heart Valve. *Scientific Reports* **2018,** *8* (1), 8187.
8. Dash, T. K.; Konkimalla, V. B., Polymeric Modification and Its Implication in Drug Delivery: Poly-ε-caprolactone (PCL) as a Model Polymer. *Molecular Pharmaceutics* **2012,** *9* (9), 2365-2379.
9. Rai, A.; Senapati, S.; Saraf, S. K.; Maiti, P., Biodegradable poly(ε-caprolactone) as a controlled drug delivery vehicle of vancomycin for the treatment of MRSA infection. *Journal of Materials Chemistry B* **2016,** *4* (30), 5151-5160.
10. Grossen, P.; Witzigmann, D.; Sieber, S.; Huwyler, J., PEG-PCL-based nanomedicines: A biodegradable drug delivery system and its application. *Journal of Controlled Release* **2017,** *260*, 46-60.
11. Chang, S. H.; Lee, H. J.; Park, S.; Kim, Y.; Jeong, B., Fast Degradable Polycaprolactone for Drug Delivery. *Biomacromolecules* **2018,** *19* (6), 2302-2307.
12. Woodruff, M. A.; Hutmacher, D. W., The return of a forgotten

polymer—Polycaprolactone in the 21st century. *Progress in Polymer Science* **2010,** *35* (10), 1217-1256.

13. Sarasam, A.; Madihally, S. V., Characterization of chitosan–polycaprolactone blends for tissue engineering applications. *Biomaterials* **2005,** *26* (27), 5500-5508.

14. Navarro-Baena, I.; Sessini, V.; Dominici, F.; Torre, L.; Kenny, J. M.; Peponi, L., Design of biodegradable blends based on PLA and PCL: From morphological, thermal and mechanical studies to shape memory behavior. *Polymer Degradation and Stability* **2016,** *132*, 97-108.

15. García Cruz, D. M.; Gomez Ribelles, J. L.; Salmerón Sánchez, M., Blending polysaccharides with biodegradable polymers. I. Properties of chitosan/polycaprolactone blends. *Journal of Biomedical Materials Research Part B: Applied Biomaterials* **2008,** *85B* (2), 303-313.

16. Narayanan, G.; Gupta, B. S.; Tonelli, A. E., Poly(ε-caprolactone) Nanowebs Functionalized with α- and γ-Cyclodextrins. *Biomacromolecules* **2014,** *15* (11), 4122-4133.

17. Jing, Q.; Law, J. Y.; Tan, L. P.; Silberschmidt, V. V.; Li, L.; Dong, Z., Preparation, characterization and properties of polycaprolactone diol-functionalized multi-walled carbon nanotube/thermoplastic polyurethane composite. *Composites Part A: Applied Science and Manufacturing* **2015,** *70*, 8-15.

18. Trollsås, M.; Lee, V. Y.; Mecerreyes, D.; Löwenhielm, P.; Möller, M.; Miller, R. D.; Hedrick, J. L., Hydrophilic Aliphatic Polyesters: Design, Synthesis, and Ring-Opening Polymerization of Functional Cyclic Esters. *Macromolecules* **2000,** *33* (13), 4619-4627.

19. Gautier, S.; D'Aloia, V.; Halleux, O.; Mazza, M.; Lecomte, P.; Jérôme, R., Amphiphilic copolymers of ε-caprolactone and γ-substituted ε-caprolactone. Synthesis and functionalization of poly(D,L-lactide) nanoparticles. *Journal of Biomaterials Science, Polymer Edition* **2003,** *14* (1), 63-85.

20. Mecerreyes, D.; Humes, J.; Miller, R. D.; Hedrick, J. L.; Detrembleur, C.; Lecomte, P.; Jérôme, R.; San Roman, J., First example of an unsymmetrical difunctional monomer polymerizable by two living/controlled methods. *Macromolecular Rapid Communications* **2000,** *21* (11), 779-784.

21. Jazkewitsch, O.; Mondrzyk, A.; Staffel, R.; Ritter, H., Cyclodextrin-Modified Polyesters from Lactones and from Bacteria: An Approach to New Drug Carrier Systems. *Macromolecules* **2011,** *44* (6), 1365-1371.

22. Habnouni, S. E.; Darcos, V.; Coudane, J., Synthesis and Ring Opening Polymerization of a New Functional Lactone, α-Iodo-ε-caprolactone: A Novel Route to Functionalized Aliphatic Polyesters. *Macromolecular Rapid Communications* **2009,** *30* (3), 165-169.

23. Lenoir, S.; Riva, R.; Lou, X.; Detrembleur, C.; Jérôme, R.; Lecomte, P., Ring-Opening Polymerization of α-Chloro-ε-caprolactone and Chemical Modification of Poly(α-chloro-ε-caprolactone) by Atom Transfer Radical Processes. *Macromolecules* **2004,** *37* (11), 4055-4061.

24. Chen, T.; Cai, T.; Jin, Q.; Ji, J., Design and fabrication of functional polycaprolactone. *E-Polymers E-Polymers* **2015,** *15* (1), 3-13.

25. Hao, J.; Servello, J.; Sista, P.; Biewer, M. C.; Stefan, M. C., Temperature-sensitive aliphatic polyesters: synthesis and characterization of γ-substituted caprolactone monomers and polymers. *Journal of Materials Chemistry* **2011,** *21* (29), 10623-10628.

26. Winkler, M.; Raupp, Y. S.; Köhl, L. A. M.; Wagner, H. E.; Meier, M. A. R., Modified Poly(ε-caprolactone)s: An Efficient and Renewable Access via Thia-Michael Addition and Baeyer–Villiger Oxidation. *Macromolecules* **2014,** *47* (9), 2842-2846.

27. Seyednejad, H.; Ghassemi, A. H.; van Nostrum, C. F.; Vermonden, T.; Hennink, W. E., Functional aliphatic polyesters for biomedical and pharmaceutical applications. *Journal of Controlled Release* **2011,** *152* (1), 168-176.

28. Anjan Kumar, M.; Utpal, J.; Prabal Kumar, M.; Guru Prasad, M., Synthesis and evaluation of MePEG-PCL diblock copolymers: surface properties and controlled release behavior. *Progress in Biomaterials* **2015,** *4* (2-4), 89-100.

29. Xu, C.; Lee, W.; Dai, G.; Hong, Y., Highly Elastic Biodegradable Single-Network Hydrogel for Cell Printing. *ACS Applied Materials & Interfaces* **2018,** *10* (12), 9969-9979.

30. Durmaz, H.; Sanyal, A.; Hizal, G.; Tunca, U., Double click reaction strategies for polymer conjugation and post-functionalization of polymers. *Polymer Chemistry* **2012,** *3* (4), 825-835.

31. Guo, B.; Finne-Wistrand, A.; Albertsson, A.-C., Universal Two-Step Approach to Degradable and Electroactive Block Copolymers and Networks from Combined Ring-Opening Polymerization and Post-Functionalization via Oxidative Coupling Reactions. *Macromolecules* **2011,** *44* (13), 5227-5236.

32. Wang, H.; Synatschke, C. V.; Raup, A.; Jérôme, V.; Freitag, R.; Agarwal, S., Oligomeric dual functional antibacterial polycaprolactone. *Polymer Chemistry* **2014,** *5* (7), 2453-2460.

33. Feng, Y.; Behl, M.; Kelch, S.; Lendlein, A., Biodegradable Multiblock Copolymers Based on Oligodepsipeptides with Shape-Memory Properties. *Macromolecular Bioscience* **2009,** *9* (1), 45-54.

34. Zhu, H.; Deng, G.; Chen, Y., Amphiphilic polymer brushes with alternating PCL and PEO grafts through radical copolymerization of styrenic and maleimidic macromonomers. *Polymer* **2008,** *49* (2), 405-411.

35. Zhang, M.; Liu, H.; Shao, W.; Miao, K.; Zhao, Y., Synthesis and Properties of Multicleavable Amphiphilic Dendritic Comblike and Toothbrushlike Copolymers Comprising Alternating PEG and PCL Grafts. *Macromolecules* **2013,** *46* (4), 1325-1336.

36. Li, S.; Ye, C.; Zhao, G.; Zhang, M.; Zhao, Y., Synthesis and properties of monocleavable amphiphilic comblike copolymers with alternating PEG and PCL grafts. *Journal of Polymer Science Part A: Polymer Chemistry* **2012,** *50* (15), 3135-3148.

37. Choi, E.-J.; Kim, C.-H.; Park, J.-K., Synthesis and Characterization of Starch-g-Polycaprolactone Copolymer. *Macromolecules* **1999,** *32* (22), 7402-7408.

38. Rieger, J.; Van Butsele, K.; Lecomte, P.; Detrembleur, C.; Jérôme, R.; Jérôme, C., Versatile functionalization and grafting of poly(ε-caprolactone) by Michael-type addition. *Chemical Communications* **2005,** (2), 274-276.

39. Molina, B. G.; Bendrea, A. D.; Cianga, L.; Armelin, E.; del Valle, L. J.; Cianga, I.; Alemán, C., The biocompatible polythiophene-g-polycaprolactone copolymer as an efficient dopamine sensor platform. *Polymer Chemistry* **2017,** *8* (39), 6112-6122.

40. Nomura, N.; Akita, A.; Ishii, R.; Mizuno, M., Random Copolymerization of ε-Caprolactone with Lactide Using a

Homosalen−Al Complex. *Journal of the American Chemical Society* **2010,** *132* (6), 1750-1751.
41. Ali Mohamed, A.; Salhi, S.; Abid, S.; El Gharbi, R.; Fradet, A., Quasi-alternating polyesteramides from ε-caprolactone and α-amino acids. *Journal of Applied Polymer Science* **2016,** *133* (46).
42. Ali Mohamed, A.; Salhi, S.; Abid, S.; El Gharbi, R.; Fradet, A., Random and quasi-alternating polyesteramides deriving from ε-caprolactone and β-alanine. *European Polymer Journal* **2014,** *53*, 160-170.
43. Lee, S. C.; Kang, S. W.; Kim, C.; Kwon, I. C.; Jeong, S. Y., Synthesis and characterization of amphiphilic poly(2-ethyl-2-oxazoline)/poly(ε-caprolactone) alternating multiblock copolymers. *Polymer* **2000,** *41* (19), 7091-7097.
44. Malhotra, M.; Surnar, B.; Jayakannan, M., Polymer Topology Driven Enzymatic Biodegradation in Polycaprolactone Block and Random Copolymer Architectures for Drug Delivery to Cancer Cells. *Macromolecules* **2016,** *49* (21), 8098-8112.
45. Sharma, B.; Keul, H.; Höcker, H.; Loontjens, T.; Benthem, R. v., Synthesis and characterization of alternating poly(amide urethane)s from ε-caprolactone, diamines and diphenyl carbonate. *Polymer* **2005,** *46* (6), 1775-1783.
46. Li, G.; Li, D.; Niu, Y.; He, T.; Chen, K. C.; Xu, K., Alternating block polyurethanes based on PCL and PEG as potential nerve regeneration materials. *Journal of Biomedical Materials Research Part A* **2014,** *102* (3), 685-697.
47. Xu, F. J.; Wang, Z. H.; Yang, W. T., Surface functionalization of polycaprolactone films via surface-initiated atom transfer radical polymerization for covalently coupling cell-adhesive biomolecules. *Biomaterials* **2010,** *31* (12), 3139-3147.
48. Parrish, B.; Breitenkamp, R. B.; Emrick, T., PEG- and Peptide-Grafted Aliphatic Polyesters by Click Chemistry. *Journal of the American Chemical Society* **2005,** *127* (20), 7404-7410.
49. Gokhale, S.; Xu, Y.; Joy, A., A Library of Multifunctional Polyesters with "Peptide-Like" Pendant Functional Groups. *Biomacromolecules* **2013,** *14* (8), 2489-2493.
50. Liu, Q.; Wang, C.; Guo, Y.; Peng, C.; Narayanan, A.; Kaur, S.; Xu, Y.; Weiss, R. A.; Joy, A., Opposing Effects of Side-Chain Flexibility and Hydrogen Bonding on the Thermal, Mechanical, and Rheological Properties of Supramolecularly Cross-Linked Polyesters. *Macromolecules* **2018,** *51* (22), 9294-9305.
51. Wu, H.; Zhu, H.; Zhuang, J.; Yang, S.; Liu, C.; Cao, Y. C., Water-Soluble Nanocrystals Through Dual-Interaction Ligands. *Angewandte Chemie International Edition* **2008,** *47* (20), 3730-3734.
52. Standard Test Method for Tensile Properties of Plastics.
53. Peng, C.; Joy, A., Alternating and random-sequence polyesters with distinct physical properties. *Polymer Chemistry* **2017,** *8* (15), 2397-2404.
54. Jeffrey, G. A.; Saenger, W., *Hydrogen bonding in biological structures*. Springer: Berlin, 1994.
55. Kennedy, M. A.; Peacock, A. J.; Failla, M. D.; Lucas, J. C.; Mandelkern, L., Tensile Properties of Crystalline Polymers: Random Copolymers of Ethylene. *Macromolecules* **1995,** *28* (5), 1407-1421.
56. Middleton, L. R.; Szewczyk, S.; Azoulay, J.; Murtagh, D.; Rojas, G.; Wagener, K. B.; Cordaro, J.; Winey, K. I., Hierarchical Acrylic Acid Aggregate Morphologies Produce Strain-Hardening in Precise Polyethylene-Based Copolymers. *Macromolecules* **2015,** *48* (11), 3713-3724.
57. Liu, X.-b.; Zhao, Y.-f.; Fan, X.-h.; Chen, E.-q., Crystal orientation and melting behavior of poly(ε-Caprolactone) under one-dimensionally "hard" confined microenvironment. *Chinese Journal of Polymer Science* **2013,** *31* (6), 946-958.
58. White, J. L.; Spruiell, J. E., The specification of orientation and its development in polymer processing. *Polymer Engineering & Science* **1983,** *23* (5), 247-256.
59. Schrauwen, B. A. G.; Breemen, L. C. A. v.; Spoelstra, A. B.; Govaert, L. E.; Peters, G. W. M.; Meijer, H. E. H., Structure, Deformation, and Failure of Flow-Oriented Semicrystalline Polymers. *Macromolecules* **2004,** *37* (23), 8618-8633.
60. Ragaert, K.; De Baere, I.; Degrieck, J.; Cardon, L., *Bulk Mechanical Porperties of Thermoplastic PCL*. 2014.
61. Buschow, K. H. J., *Encyclopedia of materials: science and technology* Elsevier: Amsterdam [etc.], 2001.
62. Jenkins, M., *DURABILITY AND RELIABILITY OF MEDICAL POLYMERS*. WOODHEAD: [S.l.], 2017.
63. Li, J.; Rothstein, S. N.; Little, S. R.; Edenborn, H. M.; Meyer, T. Y., The Effect of Monomer Order on the Hydrolysis of Biodegradable Poly(lactic-co-glycolic acid) Repeating Sequence Copolymers. *Journal of the American Chemical Society* **2012,** *134* (39), 16352-16359.

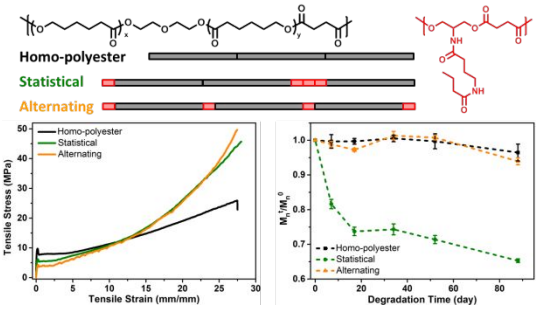

PCL analogues prepared by facile polycondensation copolymerization in statistical and alternating motifs demonstrate corresponding effects on their thermal, physical and mechanical properties.